DE GRUYTER Biomed. Eng.-Biomed. Tech. 2025; 70(5): 403–413

Valentina Betti*, Halldór Jónsson Jr, Luca Cristofolini, Magnús Kjartan Gíslason and Paolo Gargiulo

# A computational 3D analysis for assessing bone remodeling following total hip arthroplasty: a longitudinal study spanning six years

https://doi.org/10.1515/bmt-2023-0643
Received December 14, 2023; accepted June 6, 2025;
published online July 9, 2025

**Abstract**

**Objectives:** This study aimed to enhance the comprehension of volumetric bone mineral density (vBMD) changes following Total Hip Arthroplasty (THA) by establishing a protocol to (i) precisely locate alterations in the proximal femur in three dimensions and (ii) evaluate these changes over an extended period.

**Methods:** Twelve individuals who underwent unilateral THA, using either cemented or uncemented prostheses, were recruited. CT-scans of the proximal femur were acquired at three distinct time points: 24 h, 1 and 6 years post-surgery. Utilizing the acquired data, 3D models of the proximal femur were generated, and a novel algorithm was developed to categorize them into Gruen zones. Comparative analysis of density values among the three sets of scans allowed the calculation of bone density gains/losses for the entire proximal femur and specific regions.

**Results:** A lower trabecular bone quantity was observed in the cemented group compared to the uncemented cohort, with discernible differences in vBMD evolution observed in the overall femur and certain Gruen zones. Noteworthy inter-patient variability was evident, ranging from physiological bone remodeling to unexpected increases/decreases in vBMD (e.g.,+340 % after one year).

**Conclusions:** This analysis proves to be a valuable tool to understand the long-term vBMD evolution in THA patients.

***Corresponding author: Valentina Betti**, Laboratory of Biomechanics, Department of Industrial Engineering, University of Bologna, Bologna, Italy, E-mail: valentina.betti9@unibo.it. https://orcid.org/0000-0002-8872-8033
**Halldór Jónsson Jr**, Department of Orthopaedics, Landspitali University Hospital, Reykjavik, Iceland
**Luca Cristofolini,** Laboratory of Biomechanics, Department of Industrial Engineering, University of Bologna, Bologna, Italy
**Magnús Kjartan Gíslason,** Institute of Biomedical and Neural Engineering, Department of Engineering, Reykjavik University, Reykjavik, Iceland
**Paolo Gargiulo,** Institute of Biomedical and Neural Engineering, Department of Engineering, Reykjavik University, Reykjavik, Iceland; and Department of Science, Landspitali University Hospital, Reykjavik, Iceland

**Keywords:** bone remodelling; total hip arthroplasty; Gruen zones; longitudinal study

## Introduction

Bone remodelling is a continuous process by which bone resorption by osteoclasts is followed by bone formation by osteoblasts so that bone may maintain its strength and mineral homeostasis. As explained by Wolff's law, bone remodels itself in response to the load it is subjected to and such mechanism varies within and among the different bones of the skeleton [1–3]. This variation depends on various factors (e.g. age, sex, pathologies, activity level) [4]. In case of a total hip arthroplasty (THA), other factors affect bone remodelling, such as the size and the geometry of the implant [5, 6]. Another factor that plays a key role in how bone remodels is the fixation method and the mechanism of load transfer between the implant and the host bone [7, 8]. Such fixation can be done either by using the cement or by relying on the interference between the stem and the femur. In the cemented prostheses, the stem has a thinner shape and it is surrounded by a layer of cement that distributes the stress in a more physiological way compared to uncemented prostheses [9, 10]. In both cases, the insertion of the stem into the femoral canal leads to changes to the stress experienced by the bone tissue [11, 12]. Such stresses are primarily transferred by the stiffer material, namely the prosthesis [13]. This leads to a bone mass redistribution at the bone-implant interface caused by the stress-shielding phenomenon [14]. Indeed, after the insertion of the stem, the stresses in the entire periprosthetic femur are redistributed. As a consequence, the bone remodels to adapt to the new environment by changing its bone mass, in particular around the proximal area [15].

Research on bone remodelling around the prosthesis over time is a key element to locate where the changes in bone mineral density (BMD) are more likely to occur [16, 17]. Indeed, despite being one of the most successful surgeries, there are a few cases in which the interaction between the bone and the prosthesis does not work as planned, leading to a non-physiological bone remodelling, and in worst case scenario to an implant failure or periprosthetic fractures because of periprosthetic bone loss [18, 19]. Various studies regarding this topic have been conducted throughout the years, with a follow-up period ranging from 18 months to 5 years post-operation [20–22]. In all these studies, the bone mineral density was measured in regions of interest surrounding the femoral component, according to the standard Gruen analysis protocol [23]. Results show that the most significant bone loss occurs in the proximal area, both if a cemented or an uncemented prosthesis was implanted [24, 25]. Regarding the distal area, bone mineral density changes are highly dependent on the size and stiffness of the implant, along with the proper placement of the stem in the intra-medullary cavity [21, 26].

In all of these studies, the BMD was measured with dual-energy X-ray absorptiometry (DXA); this is however a projectional technique, which only measures density in terms of area (in $mg/cm^2$) and not the volumetric density (in $mg/cm^3$). Therefore, DXA-based methods rely on assumptions regarding bone mineral distribution in the third dimension, given that bone remodelling is a 3D mechanism [27]. In other research, bone remodelling was investigated by using post-operative CT scans [28–30]. To the authors' best knowledge, just one study on four patients with uncemented prostheses has a follow-up time greater than two years, but the BMD changes were analysed in detail just for five slices of interest [31]. A quantitative information for the whole proximal femur would be useful to use THA patients as "labs" to better understand the bone remodelling mechanism in the long run. Moreover, it would be helpful in order to monitor the few cases where a failure or a non-physiological behaviour is observed or suspected. In this regard, however, no research has been carried out.

The main aim of this work was to improve the understanding of the bone remodelling process in THA patients in the long-term, by using a 3D approach. The specific aims of this study were: i) to develop a methodology to quantitatively assess the volumetric bone mineral density (vBMD) in a longitudinal study, ii) to localise these changes in the seven standard Gruen zones, and iii) to investigate the bone remodelling mechanism 24 h, 1 year and 6 years post THA. To reach this goal, CT scans from a longitudinal study were used to evaluate the vBMD over time.

# Methods

The pipeline to evaluate the trend of vBMD is reported in Figure 1 and described in detail below.

## Data collection

***Patient recruitment***. The methodology to evaluate the vBMD changes was carried out on twelve subjects undergoing primary unilateral THA, either in uncemented or cemented setting. The average age was 63±8 years. Information about the cohort distribution is shown in Table 1. The same type of femoral stem was used for each group. For the uncemented group, the CLS Spotorno stem, made from a titanium alloy, was used and the MS 30 stem, made from stainless steel, was used for the cemented group. Ethical approval was obtained from the local bioethics committee.

***CT acquisition and calibration***. Spiral CT scans of the patients' femurs were taken, covering the region from the front upper part of the pelvic bone to the lower part of the thigh at intervals of 24 h, 1 year, and 6–7 years after the surgical procedure. For the initial pair of scans, a Philips Brilliance 64 Spiral-CT machine was used (X-ray tube current: 249 mA, kilovoltage peak: 120 kVp, and resolution: [0.5 × 0.5 × 1] mm). For the CT-scans acquired 6–7 years after THA, a Toshiba Aquilion PRIME was used (X-ray tube current: 600 mA, kilovoltage peak: 120 kVp, and resolution: [0.3 × 0.45 × 0.5] mm). The scans were calibrated using a calibration phantom (Micro-CT HA phantom, GmbH, Möhrendorf, Germany) to find the mathematical relationship that converts the CT-scan values (in [HU]) into apparent density, i.e. vBMD (in [g/cm$^3$]). The relationship for the Philips scanner was already been calculated in a previous study [32]:

$$vBMD_1 = -8 \cdot 10^{-8} \cdot HU^2 + 0.0006 \cdot HU + 0.9456 \qquad (1)$$

The calibration for the Toshiba scanner was carried out at the time of the study, and was found to be:

$$vBMD_2 = 0.000494 \cdot HU + 1.1 \qquad (2)$$

## 3D Modelling

The whole process developed to obtain the 3D models of the femurs was carried out through the software platform *Mimics* (Materialise NV, Leuven, Belgium).

***Scatter reduction.*** In order to reduce the effects of metal artefacts on the estimated HU values, a scatter reduction was performed on each CT image from the three datasets (post 24 h, post 1 y and post 6 y). By setting the filtering strength to 100 %, artefacts were reduced iteratively for each slice (Figure 2).

***Re-slicing***. The positioning of the patient within the CT scanner may vary significantly, not only between different patients but also within the same individual across the three consecutive datasets. Notably, varying degrees of abduction/adduction and internal/external rotation are discernible in multiple CT scans. Consequently, a realignment procedure was necessary to orientate the legs uniformly along a shared digital scanning axis, thereby streamlining the comparison

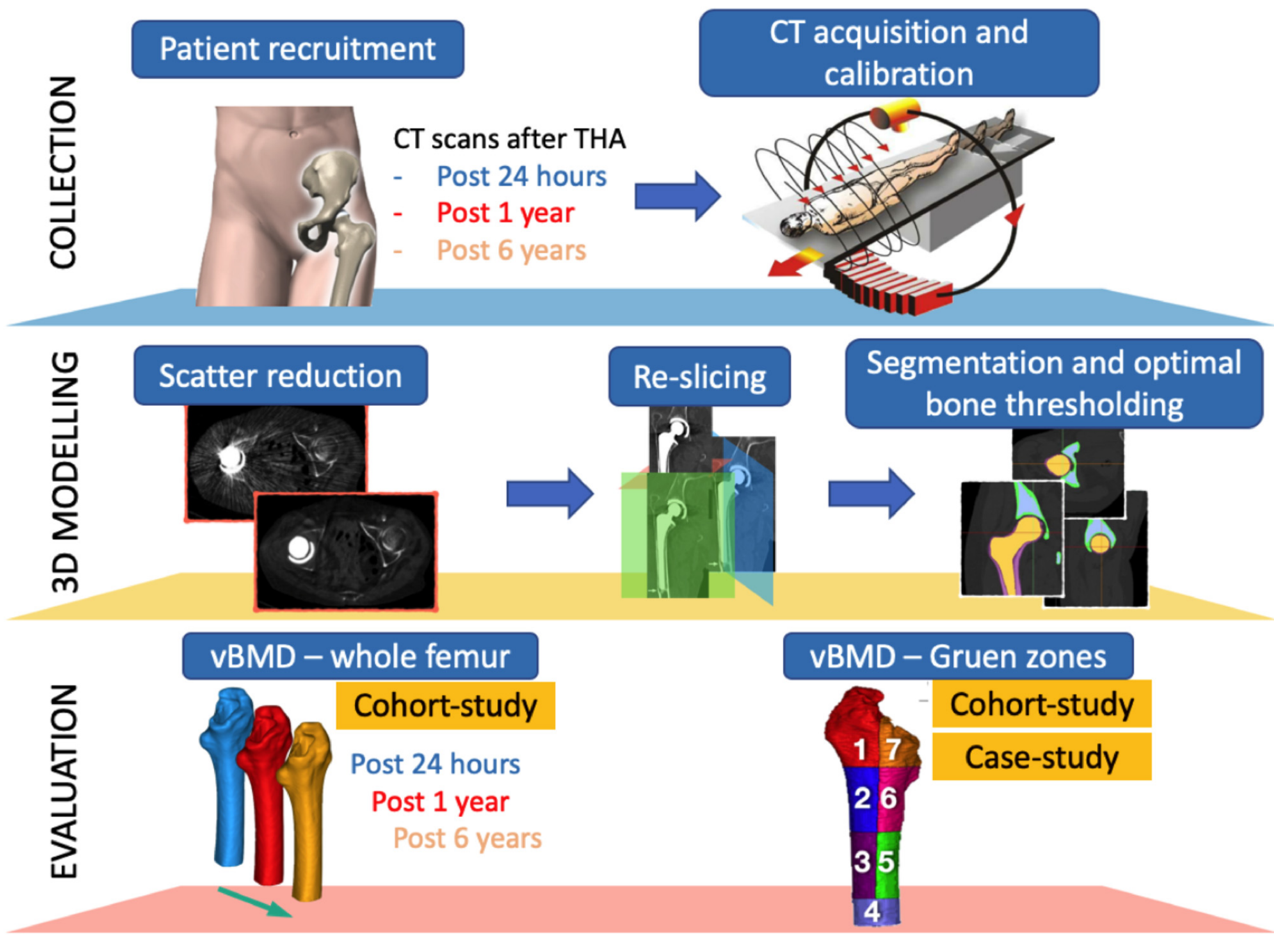


**Figure 1:** Study workflow.

**Table 1:** Information about study participants. "Age" refers to the age of subjects when primary THA was performed.

| Patient N° | Sex | Age | Implant | Operated side |
|---|---|---|---|---|
| 1 | Female | 70 | Cemented | Left |
| 2 | Female | 74 | Cemented | Left |
| 3 | Female | 75 | Cemented | Left |
| 4 | Female | 63 | Cemented | Right |
| 5 | Male | 65 | Cemented | Right |
| 6 | Female | 57 | Uncemented | Right |
| 7 | Female | 63 | Uncemented | Right |
| 8 | Male | 50 | Uncemented | Left |
| 9 | Male | 52 | Uncemented | Right |
| 10 | Male | 56 | Uncemented | Right |
| 11 | Male | 59 | Uncemented | Left |
| 12 | Male | 67 | Uncemented | Right |

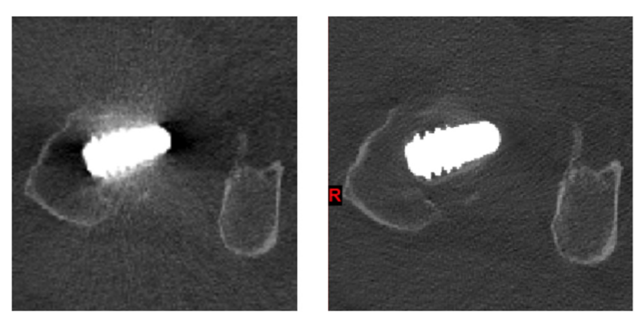

**Figure 2:** Pre- and post-processed CT-scans. On the left, a CT slice before the artefact reduction; on the right, the same slice after the application of the "Reduce scatter" algorithm.

of the same thigh bones across different time points. An alignment of body orientation was achieved by drawing a straight line passing through the longitudinal axis of the femur. Areas of interest were thus cropped, namely the operated femur and the unoperated femur. To allow an easier comparison between the three consecutive datasets, in the operated leg the line was traced starting from 2 cm below the distal part of the stem's tip and ending 5 cm above the proximal extremity of the implant. Since no implant was present for the contra-lateral leg, the same distances measured for the operated leg were used.

Moreover, pixel size was uniformed, since this parameter could be different between post 24 h, post 1 y and post 6 y CT-scans. In order to provide the best result in terms of resolution, the lowest value of the three consecutive datasets was chosen as standard and applied to the other two images.

***Segmentation and optimal bone thresholding.*** A segmentation based on thresholding was performed to isolate both the operated and the contra-lateral femur in the three datasets.

Different thresholds have been used in the literature, without a univocal standard to define this specific range. In this protocol, the choice of the higher value of the threshold was straightforward, since the densities of the metal and the bone always differed significantly, so 2999 HU was chosen by looking at the histogram. Instead, the choice of the lower value was troublesome, given that the residual scatter and partial volume effects (PVEs) made the distinction between trabecular bone and soft tissues more difficult. In order to choose the optimal value to start with, four masks were created starting from different thresholds: 148 HU, 226 HU, 300 HU, and 350 HU. Indeed, by converting these values in apparent density through the calibration formulas, acceptable values for bone mineral density were found, according to previous studies [33–35].

Ten biomedical engineers were then asked to perform the post-editing of these four masks. Five subjects of the group were already familiar with the segmentation process ($g_{tr}$), while the other five were just trained at the time of the experiment ($g_{un}$). To ensure the reproducibility of the experiment, a detailed protocol was provided, which required them to remove some eventual pixel of noise outside the femur, the fill of the inner areas, and the Boolean subtraction between the masks of the bone and the prosthesis respectively. The uncertainty error [%] in the volume of the final masks of the femurs was calculated as:

$$Err_{i_{\%}} = \frac{|V_{op_i} - V_r| + |V_r - V_{op_i}|}{V_r} \cdot 100 \qquad (3)$$

where $V_{op_i}$ and $V_r$ are respectively the volume of the mask of each operator and the volume of the mask of the first author set as the reference mask. The average error ($Err_{\mu_{\%}}$) was then calculated for the four masks.

Two statistical analyses were then performed:
– Mann–Whitney U test, to assess any statistical variance between the two groups;
– Intraclass Correlation (ICC(3,1)), to assess the reproducibility of the measurement.

Following the selection of the optimal threshold, an additional measurement was taken to handle the existence of the cement layer on the 3D masks of the patients who underwent a cemented prosthesis procedure. The mask of the implant was isolated ([2500 - max] HU), and dilated by 3 pixels throughout the respective morphology operation, so to consider ~2 mm of space between the prosthesis and the bone. Then a Boolean subtraction was performed between the mask of the bone on the operated side and this dilated implant, thus thinning the former.

## Evaluation

In order to evaluate the vBMD variations between consecutive datasets, the masks of the operated and the contra-lateral femurs were imported into *Matlab* (Mathworks Inc, vers. 2021a). To better localise the changes in bone density, a specific evaluation of bone remodelling throughout the years was investigated by splitting the femurs in the seven Gruen zones. An algorithm was developed to realign the femur through the longitudinal axis, and then dividing the bone between medial and lateral. Through the identification of the tip of the lesser trochanter and the distal tip of the prosthesis, the Gruen zones were automatically separated for each femur.

***Longitudinal vBMD assessment one and six years post-operatively.*** Three different analyses were then performed:
– a cohort-study for the whole proximal femur in patients with THA (both cemented and uncemented);
– a cohort-study for the Gruen zones of the operated femur, so as to analyse the trend of vBMD in such specific areas;
– a patient-specific approach for the Gruen zones, to report some examples of the bone remodelling mechanism.

# Results

## Segmentation and optimal bone thresholding

The average error calculated for the four masks with Eq.(3) is reported in Table 2. The mean error computed for the trained and the untrained groups did not differ significantly (p>0.1).

Regarding the ICC(3,1) analysis, the values obtained with thresholds 148, 226, and 350 HU are indicative of poor reliability (Table 3). As for the 300 HU threshold, the level of reliability can be regarded as moderate (p=0.05).

**Table 2:** Error [%] for the four masks obtained for the four different thresholds (Eq.(3)).

| Threshold [HU] | 148 | | 226 | | 300 | | 350 | |
|---|---|---|---|---|---|---|---|---|
| | $g_{tr}$ | $g_{un}$ | $g_{tr}$ | $g_{un}$ | $g_{tr}$ | $g_{un}$ | $g_{tr}$ | $g_{un}$ |
| $Err_{1_{\%}}$ | 4.9 | 5.6 | 2.3 | 2.6 | 1.3 | 1.6 | 2.0 | 2.4 |
| $Err_{2_{\%}}$ | 5.8 | 6.0 | 2.7 | 2.5 | 1.0 | 1.9 | 1.1 | 2.4 |
| $Err_{3_{\%}}$ | 6.7 | 4.2 | 5.1 | 3.0 | 2.0 | 2.1 | 2.9 | 2.8 |
| $Err_{4_{\%}}$ | 6.2 | 6.8 | 3.3 | 5.1 | 1.6 | 2.0 | 2.3 | 2.9 |
| $Err_{5_{\%}}$ | 4.7 | 5.1 | 1.8 | 3.5 | 1.3 | 1.4 | 2.1 | 2.1 |
| $Err_{\mu_{\%}}$ | 5.6 | | 3.2 | | 1.6 | | 2.3 | |

**Table 3:** ICC(3,1) analysis performed on the volume error of the bone masks obtained using the four different segmentation thresholds (148, 226, 300, and 350 HU). ICC is the estimated intraclass correlation; LB and UB indicate the lower and upper bounds of the ICC at the chosen significance level. Bold value indicates statistical significance (p≤0.05).

| Threshold [HU] | 148 | 226 | 300 | 350 |
|---|---|---|---|---|
| LB | −0.24 | −0.24 | −0.08 | −0.19 |
| ICC | −0.23 | −0.20 | 0.56 | 0.23 |
| UB | 0.88 | 0.97 | 0.99 | 0.99 |
| p-value | 0.84 | 0.71 | **0.05*** | 0.19 |

## Longitudinal vBMD assessment one and six years post-operatively

### Cohort study: entire femurs evaluation

Volumetric bone mineral density changes in both operated and unoperated femurs were evaluated comparing the masks obtained 24 h, 1 year, and 6 years post-operatively. Figure 3 shows average values and the standard deviation for the patients with a cemented and uncemented approach separately. To obtain the percentage rate, each number of voxels corresponding to a BMD value was normalised dividing by the total volume of the mask and multiplying by 100. Moreover, a black dotted line was used to divide the density values corresponding to trabecular bone from those corresponding to cortical bone. To this aim, a threshold was chosen at 1.4310 $g/cm^3$ (670 HU), since several studies suggest this value to be in the range that best identifies the cortico-cancellous interface [36, 37]. Blue, red, and yellow distributions represent the changes for operated (Figure 3a and c) and unoperated femurs (Figure 3b and d) at 24 h, 1 year, and 6 years respectively. Data show a great variability between subjects, as shown by the relatively high standard deviation, up to ±45 %. In general, however, a lower amount of trabecular bone can be observed in the operated side (Figure 3a and c) compared to the control leg (Figure 3b and d). Furthermore, such percentage is found to be lower in the group with a cemented stem (Figure 3a), rather than the uncemented one (Figure 3c).

### Cohort study: Gruen zones evaluation

The variation in terms of vBMD frequency were assessed separately for trabecular and cortical bone, and divided for each Gruen zone. The area underlying the curve was calculated for the two types of bone in the three separate datasets, and then values from post 1 y and post 6 y were normalised by post 24 h value using the below formula:

$$BMD\ changes\ [\%] = \frac{Area_{Post\ 1y\ (or\ 6y)} - Area_{Post\ 24h}}{Area_{Post\ 24h}} \cdot 100 \quad (4)$$

The vBMD changes for the trabecular bone (shown with an asterisk) and cortical bone (shown with a circle) are reported in Figure 4 for both the cemented and uncemented group (in blue and green boxes respectively), showing the average increase/decrease rate (*y*-axis) over time (*x*-axis). Differences after one year after the THA are shown in red, while differences after six years are reported in yellow.

Even in this case, data show a wide variability between the subjects, reaching a standard deviation ±127 % in GZ 5 for the uncemented approach. Generally, a trend of reduction of cortical bone was noticed for both types of fixation six years post-operatively.

As regards the mean value of BMD between the cemented and uncemented groups, statistically significant changes (p<0.05) were found in:
- GZ2, 24 h post-operatively;
- GZ2, 1 y post-operatively;
- GZ4, 24 h post-operatively;
- GZ4, 1 y post-operatively;
- GZ5, 1 y post-operatively.

As regards the changes in time, statistically significant results (p<0.05) were only found for the uncemented group, and in particular in:
- GZ1, by comparing post-1 y and post-6 y data;
- GZ4, by comparing post-24 h and post-1 y data;
- GZ5, by comparing post-24 h and post-1 y data;
- GZ5, by comparing post-1 y and post-6 y data;
- GZ6, by comparing post-24 h and post-1 y data.

### Study cases: Gruen zones evaluation

The same analysis conducted to assess the vBMD changes over-time for the cemented and uncemented cohort shown in Figure 4 has been reported in the following section to discuss some cases of clinical interest. Four cases are

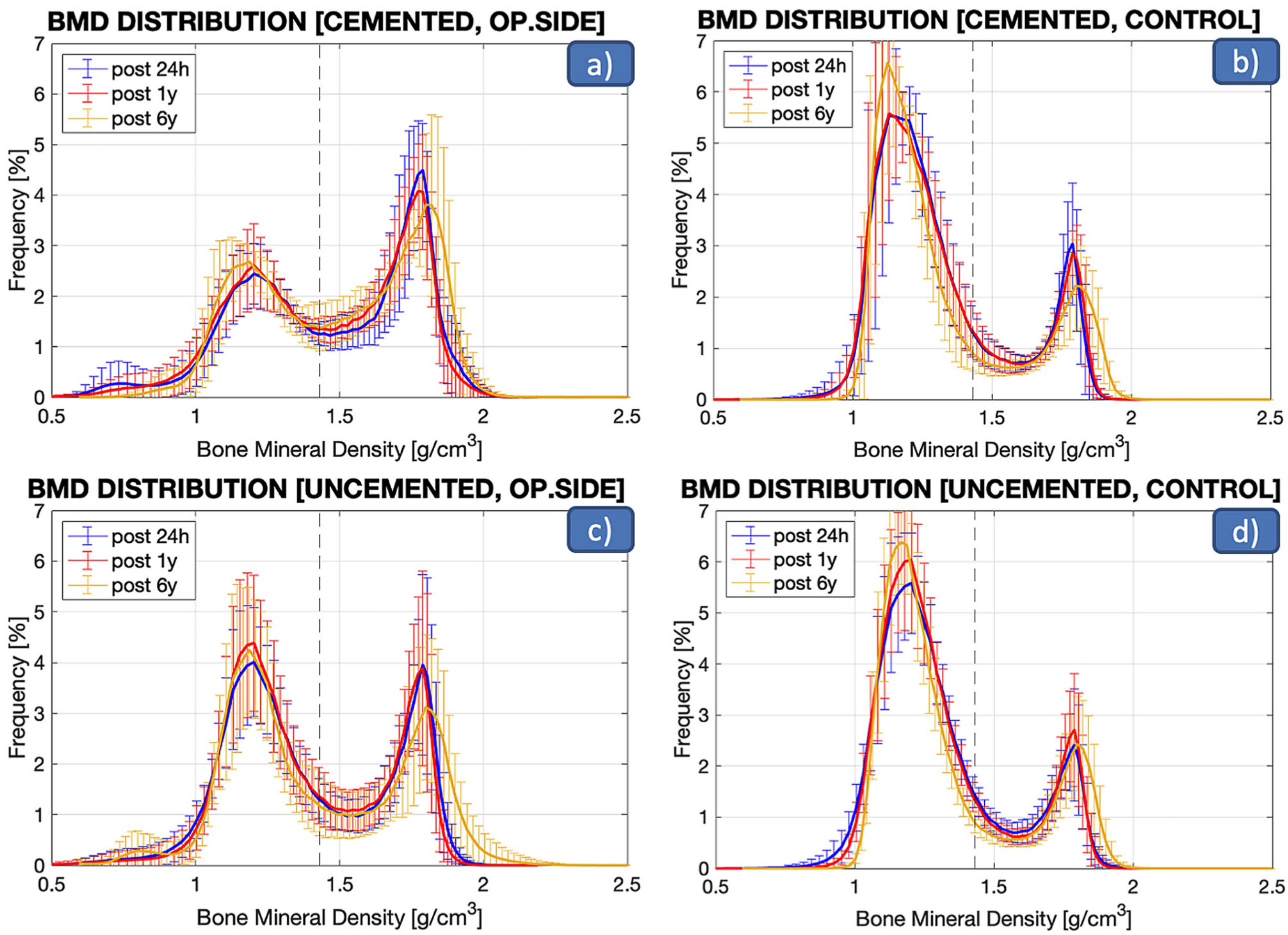


**Figure 3:** Average BMD distribution calculated for the group with a cemented prosthesis (*a* is the operated side, *b* the contro-lateral one), and uncemented prosthesis (*c* is the operated side, *d* the contro-lateral one). Each point represents the mean and standard deviation of the twelve patients. The *y*-axis displays the percentage of voxels at a specific BMD value (*x*-axis) calculated through Eq.(1) for post-24 h and post-1y data, and through Eq.(2) for post-6y data.

reported below, where the vBMD changes from 1 to 6 years post-operatively were analysed.

***Male, cemented, 65 years old.*** No significant changes were observed for trabecular bone over the six years, with the largest increase found for GZ 6 after six years (+32 %, Figure 5a). A light decrease of cortical bone was noticed overall.

***Female, cemented, 63 years old.*** An increase of trabecular bone was observed in GZs 2, 3, 5 and 6 after one year, with strong growth after six years in GZs 2 and 3 (+116 % and +174 % respectively, Figure 5b). As seen in the previous case, a light decrease of cortical bone was noticed overall.

By looking at the CT scan, a varus malalignment of the prosthesis inside the intra-medullary cavity (~5°) was detected.

***Male, uncemented, 52 years old.*** No significant changes were observed for trabecular bone over the six years, with the largest decrease found for GZ 6 after six years (–40 %, Figure 5c). A light decrease of cortical bone was noticed for GZs 3, 4, 5, and 7, while for the other GZs changes were not significant (< + 8%).

***Male, uncemented, 50 years old.*** In this case, a great increase in trabecular bone was observed after one year in GZ 3 and 5 (+143 % and +340 % respectively, Figure 5d). However, no great changes were to be found by comparing post 6 y data with post 24 h data in such areas. A similar trend was observed for the cortical bone in GZ 1.

## Discussion

The aim of this study was the development of a methodology to quantitatively assess the vBMD changes in the long run not merely in the whole femur, but also in regions of clinical interest, namely the Gruen zones. To achieve this goal, the choice of a robust threshold to obtain the 3d bone models was needed, so as to have a feasible and repeatable segmentation process. Results obtained from this method can be

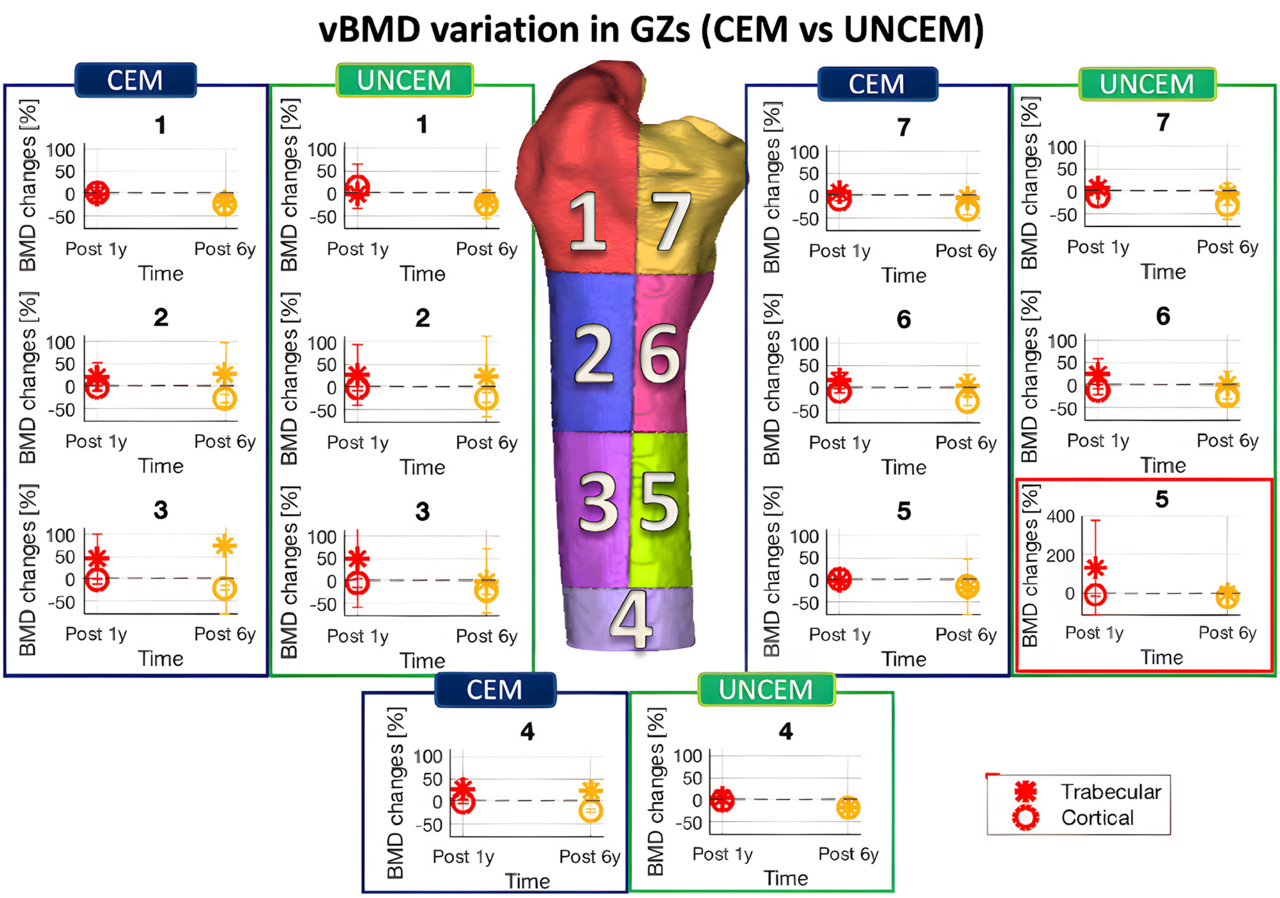


**Figure 4:** Variations [%] in voxel frequency (*y*-axis) for trabecular (asterisks) and cortical bone (circles) in the seven Gruen zones over the years (*x*-axis) (Eq.(4)). Results for the cemented group are encircled in blue boxes; for the uncemented group in green boxes. To better assess any change, *y*-axis limit is set to [−80 115] (besides GZ 5 for the uncemented group).

used for a twofold purpose: to compare any difference in terms of mineral density between the two cohort of patients (with cemented/uncemented prosthesis); to analyse the trend of bone remodelling in specific patients.

## Segmentation and optimal bone thresholding

Calculating the average uncertainty ($Err_{\mu_{\%}}$) for the four masks, the minimum value was obtained when starting with 300 HU as lower threshold. The mean error computed for the trained ($g_{tr}$) and the untrained groups ($g_{un}$) reported no statistically significant differences, showing that the operator's experience made no difference by using the protocol developed.

Results from ICC(3,1) test are in line with similar methodologies found in the literature [38, 39], and confirmed the choice of 300 HU as the optimal threshold to start the manual post-editing; indeed, the level of reliability obtained from this threshold was the highest among the group, and also the only one statistically significant.

## Longitudinal vBMD assessment one and six years post-operatively

The *in silico* methodology was used to evaluate the trend of bone remodelling in a three-dimensional way, and in the long-term (six years post-operatively).

### Cohort study: entire femurs evaluation

Concerning the vBMD distributions, the lower amount of trabecular bone found in the operated side rather than the unoperated side (Figure 3) is caused by the removal of bone stock due to the arthroplasty. Indeed, most of the bone removed to create the intra-medullary cavity to place the stem consists in trabecular bone. Moreover, the amount of bone removed was greater in the cemented group compared

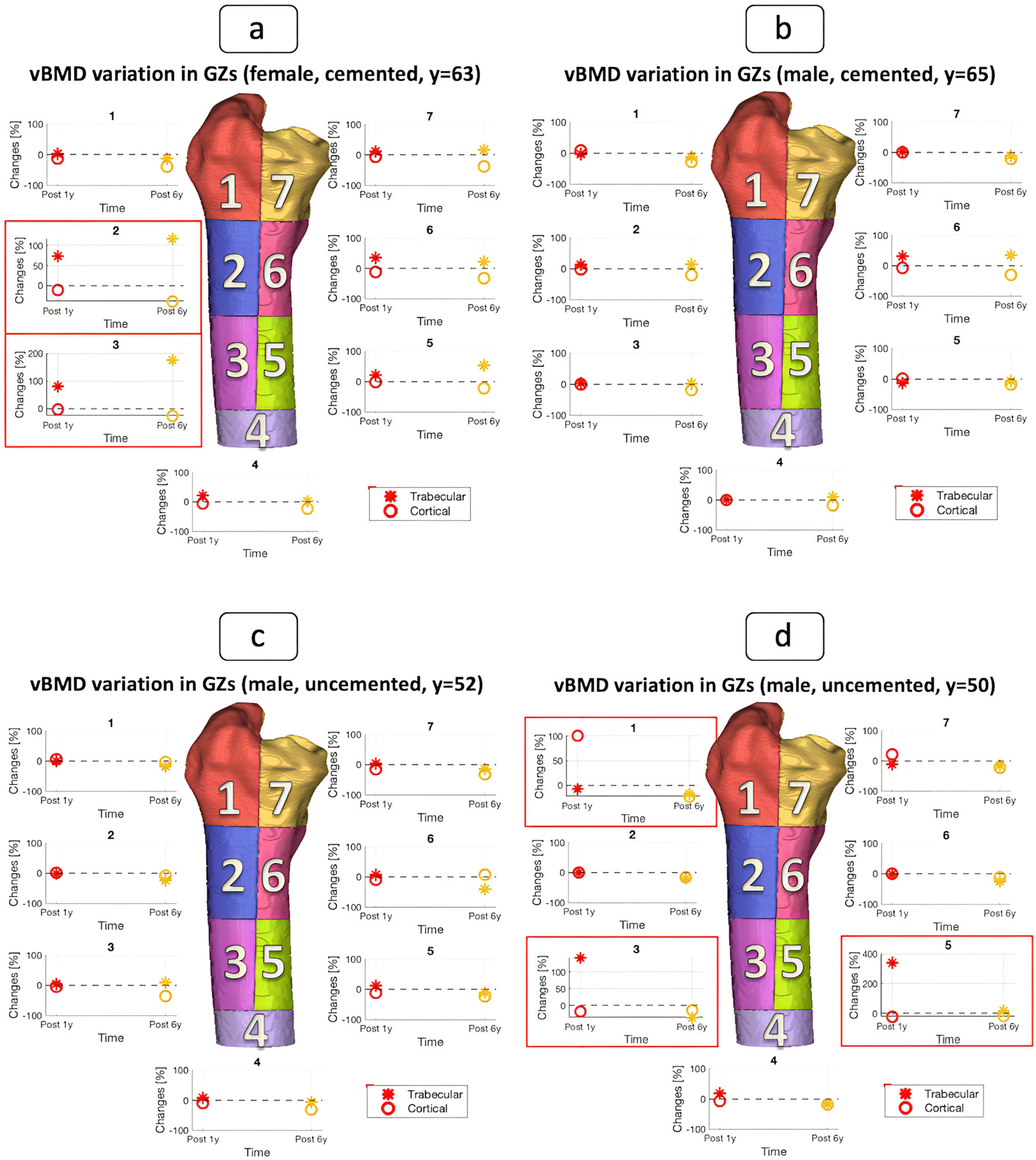


**Figure 5:** Variations [%] in voxel frequency for trabecular and cortical bone in the seven Gruen zones over the years for several subjects. a) A male subject, with a cemented implant, 65 years old at the time of operation; b) a female subject, with a cemented implant, 63 years old at the time of operation; c) a male subject, with an uncemented implant, 52 years old at the time of operation; and d) a male subject, with a uncemented implant, 50 years old at the time of operation. To better assess any change, *y*-axis limit is set to [–100 100] (besides GZ 1, 3, and 5).

to the uncemented one, since a larger cavity is required to place the cement.

**Cohort study: Gruen zones evaluation**

By looking at the vBMD changes in the seven separate Gruen zones (Figure 4), a large variability among subjects was observed, due to the high inter-patient variations in terms of sex, age and level of activity. Other studies reported a similar pattern of bone gain/loss, with the largest increases observed in GZs 2, 3 and 5 and smaller differences identified in GZs 1, 4, 6 and 7 [40].

The differences between the cemented and uncemented observed after 24 h and 1 year in GZs 2, 4, and 5 are in line with the literature, with studies observing a similar behaviour [41, 42]. About the changes in time for the uncemented group, statistically significant differences were found in GZs 4, 5, and 6, by comparing post-24 h and post 1 y-data, and in GZs 1 and 5, by comparing post-1 y and post 6 y-data. Such results are in partial agreement with other studies, since a bony development was also detected in GZ 4 [43], while the greatest loss of bone density was localised also in GZs 7 in the long-term [44]. A possible explanation for such differences relies on the limited number of THA patients that have been analysed; hopefully, the addition of more data in the future would give the possibility of drawing more conclusions about the trend of vBMD in the cemented/uncemented cohort over time.

**Study cases: Gruen zones evaluation**

In Figure 5a and b examples of vBMD changes for two patients with a cemented setting (a male and a female), were reported. Despite the same fixation method and the similar age, a different process of bone remodelling has been observed over the years among the two subjects. In the first case study, no big changes were observed, which is indicative of a stable fixation of the prosthesis. On the other hand, a different behaviour was observed in the second case, where the high increase of trabecular bone (especially in GZs 2 and 3) can be explained with the varus malalignment of the prosthesis. Such results match with other studies in the literature, proving how the bone tissue adapts to the new situation dictated by the stiffness and the alignment of the artificial joint [45].

Moreover, a physiological light decrease of cortical bone was noticed overall for both of the subjects, and it is associated with the process of aging [46].

A similar comparison for the uncemented fixation was carried out by looking at two patients with similar age (Figure 5c and d). Again, it was possible to observe a situation where no vBMD changes greater than 30 % occurred (Figure 5c), and a situation where great variations in vBMD were seen over time. A possible explanation for the increases in trabecular bone observed in GZs 3 and 5 after one year of THA relies on the damage that the femur has suffered with the broaching at the time of operation; indeed, since data were normalised by the post-24 h data, the great increase was associated to the healing of the bone. In the long run, however, the percentage of trabecular bone tended to normalise, since the bone adapted to the new prosthesis.

The increase of cortical bone observed in GZ1 one year after THA can be justified by the implant placement of the stem. Indeed, an incorrect insertion of the prosthesis can lead to an overload of the greater trochanter, thus causing an increase of BMD to overcome with such stress. In the long-term, however, the bone adapts to these loads, with a mean value of vBMD which does not differ significantly from the vBMD observed 24 h post-operation.

## Limitations

From the cohort demographics, it should be noted that the average age of the cemented group was greater than the uncemented one. This result reflects the local guidelines, for which surgeons prefer to carry out an uncemented fixation on younger subjects and a cemented fixation on the elderly ones. For such reason, it was not possible to perform a matched-cohort study with the current database. Moreover, no other tests were performed between the two groups, so as to consider some possible confounding factors. However, if this study is expanded to include balanced groups, some conclusions will be drawn about how the bone remodelling process changes depending on the fixation method.

# Conclusions

The *in silico* method presented in this study can be employed as a tool to evaluate long-term vBMD changes in the proximal femur. The protocol showed good results in terms of reproducibility ($Err_{\mu_{\%}}$) and reliability (ICC(3,1)). Such analysis is the most in-depth analysis carried out on bone quality to date, and it provides a tool for the understanding of the bone remodelling mechanism in THA patients. By increasing the number of patients, beyond that carrying out the appropriate validation of the results, it would be possible to explore whether this method is a helpful guide for the follow-up of patients where a failure of the implant is to be expected.

The methodology presented may be also deemed to decide appropriate rehabilitation strategies which can then help to prolong the time until revision surgery, thus increasing the quality of life for the patient. Indeed, it has been proven how physical decelerates bone loss associated with aging [47]. Depending on the anatomical areas where the bone loss has occurred, specific weight-bearing exercises with an impact on the bone higher than that during normal everyday activities, combined with flexibility and posture control, could be part of a rehabilitation program to prevent and manage with a bone loss.

**Acknowledgement:** The authors would like to thank J.L. and M.R. for their valuable suggestions and inspiring discussions throughout the development of this study. We are also grateful to all the members of the Institute of Biomedical and Neural Engineering in Reykjavik and the Lab of Biomechanics in Bologna for their constructive conversations, technical support, and collaborative spirit.
**Research ethics:** Project approved by the Icelandic Bioethics authority, VSN 19–186, A and B. The study was conducted in accordance with the Declaration of Helsinki.
**Informed consent:** Informed consent was obtained from all individuals included in this study, or their legal guardians or wards.
**Author contributions:** V. Betti: Conceptualization, Methodology, Formal analysis, Software, Writing - original draft; H. Jonsson Jr: Conceptualization, Data curation; L. Cristofolini: Conceptualization, Writing - review & editing; M. K. Gislason: Methodology, Software; P. Gargiulo: Conceptualization, Supervision, Resources, Project administration. The authors have accepted responsibility for the entire content of this manuscript and approved its submission.
**Use of Large Language Models, AI and Machine Learning Tools:** ChatGPT was used to improve short parts of the text and enhance the quality of existing figures.
**Conflict of interests:** The authors state no conflict of interest.
**Research funding:** This work was funded by University Hospital Landspitali (project number 972883).
**Data availability:** The raw data can be obtained on request from the corresponding author.

# References


1. Malchau H, Herberts P, Ahnfelt L. Prognosis of total hip replacement in Sweden. Follow-up of 92,675 operations performed 1978–1990. Acta Orthop Scand 1993;64:497–506.
2. Lovecchio J, Jonsdottir-Buch S, Einarsdottir G, Gislason M, Örlygsson G, Sigurjonsson O, et al. Assessment of perfusion bioreactors system using CT technology and 3D modeling methods. Biomed Tech 2014;59:302–5.
3. Esposito L, Minutolo V, Gargiulo P, Fraldi M. Symmetry breaking and effects of nutrient walkway in time-dependent bone remodeling incorporating poroelasticity. Biomech Model Mechanobiol 2022;21.
4. Lee S, Sugano N, Nakata K, Matsui M, Ohzono K. Comparison between bipolar hemiarthroplasty and THA for osteonecrosis of the femoral head. Clin Orthop Relat Res 2004;424:161–5.
5. Hayaishi Y, Miki H, Nishii T, Hananouchi T, Yoshikawa H, Sugano N. Proximal femoral bone mineral density after resurfacing total hip arthroplasty and after standard stem-type cementless total hip arthroplasty, both having similar neck preservation and the same articulation type. J Arthroplas 2007;22:1208–13.
6. Improta G, Balato G, Romano M, Carpentieri F, Bifulco P, Alessandro R M, et al. Lean six Sigma: a new approach to the management of patients undergoing prosthetic hip replacement surgery. J Eval Clin Pract 2015;21:662–72.
7. Pal B, Gupta S. The effect of primary stability on load transfer and bone remodelling within the uncemented resurfaced femur. Proc IME Part H, J Eng Med 2011;225:549–61.
8. D'Lima D, Oishi C, Petersilge W, Colwell C, Walker R. 100 cemented versus 100 noncemented stems with comparison of 25 matched pairs. Clin Orthop Relat Res 1998;348:140–8.
9. Cristofolini L, Juszczyk M, Taddei F, Field R, Rushton N, Viceconti M. Stress shielding and stress concentration of contemporary epiphyseal hip prostheses. Proc IME Part H, J Eng Med 2009;223:27–44.
10. Miladi M, Villain B, Mebtouche N, Bégué T, Aurégan JC. Interest of short implants in hip arthroplasty for osteonecrosis of the femoral head: comparative study "uncemented short" vs "cemented conventional" femoral stems. Int Orthop 2018;42:1669–74.
11. Gislason MK, Lupidio F, Jónsson H, Cristofolini L, Esposito L, Bifulco P, et al. Three dimensional bone mineral density changes in the femur over 1 year in primary total hip arthroplasty patients. Clin BioMech 2020;78:105092.
12. Esposito L, Minutolo V, Gargiulo P, Jonsson H, Gislason M, Fraldi M. Towards an app to estimate patient-specific perioperative femur fracture risk. Appl Sci 2020;10:6409.
13. Barak M, Lieberman D, Hublin JJ. A wolff in sheep's clothing: trabecular bone adaptation in response to changes in joint loading orientation. Bone 2011;49:1141–51.
14. Huiskes R, Nunamaker D. Local stresses and bone adaption around orthopedic implants. Calcif Tissue Int 1984;36:110–7.
15. Venesmaa P, Vanninen E, Miettinen H, Kröger H. Periprosthetic bone turnover after primary total hip arthroplasty measured by single-photon emission computed tomography. Scand J Surg: SJS: Off Organ Finnish Surg Soc Scand Surg Soc 2012;101:241–8.
16. Recenti M, Ricciardi C, Aubonnet R, Esposito L, Jónsson H, Gargiulo P. A regression approach to assess bone mineral density of patients undergoing total hip arthroplasty through gait analysis. In: 2020 IEEE International Symposium on Medical Measurements and Applications (MeMeA), Bari, Italy. IEEE; 2020:1–6 pp.
17. Gargiulo P, Edmunds K, Gislason M, Latour C, Hermannsson S, Esposito L, et al. Patient-specific mobility assessment to monitor recovery after total hip arthroplasty. Proc IME Part H, J Eng Med 2018; 232(10). https://doi.org/10.1177/0954411918797971.
18. Mehran N, North W, Laker M. Failure of a modular hip implant at the stem-sleeve interface. Orthopedics 2013;36:978–81.
19. Peitgen D, Innmann M, Merle C, Gotterbarm T, Moradi B, Streit M. Periprosthetic bone mineral density around uncemented titanium

stems in the second and third decade after total hip arthroplasty: a DXA study after 12, 17 and 21 years. Calcif Tissue Int 2018;10:103.
20. Sychterz CJ, Engh CA. The influence of clinical factors on periprosthetic bone remodeling. Clin Orthop Relat Res 1996;322.
21. Albanese CV, Rendine M, Palma FD, Impagliazzo A, Falez F, Postacchini F, et al. Bone remodelling in THA: a comparative DXA scan study between conventional implants and a new stemless femoral component. A preliminary report. HIP Int 2006;16:9–15.
22. Behrens BA, Bouguecha A, Lerch M, Windhagen H, Mahlme A. Influence of hip prosthesis size and its coating area on bone remodeling. IEEE Trans NanoBiosci 2017;16:703–7.
23. Gruen T, McNeice G, Amstutz H. Modes of failure" of cemented stem-type femoral components: a radiographic analysis of loosening. Clin Orthop Relat Res 1979;141:17–27.
24. Kröger H, Miettinen H, Arnala I, Koski E, Rushton N, Suomalainen O. Evaluation of periprosthetic bone using dual-energy X-ray absorptiometry: precision of the method and effect of operation on bone mineral density. J Bone Miner Res 2009;11:1526–30.
25. Nishii T, Sugano N, Masuhara K, Shibuya T, Ochi T, Tamura S. Longitudinal evaluation of time related bone remodeling after cementless total hip arthroplasty. Clin Orthop Relat Res 1997;339: 121–31.
26. Engh CA, Sychterz C, Engh C. Factors affecting femoral bone remodeling after cementless total hip arthroplasty. J Arthroplast 1999; 14:637–44.
27. Alawi M, Begum A, Harraz M, Alawi H, Bamagos S, Yaghmour A, et al. Dual-energy X-Ray absorptiometry (DEXA) scan versus computed tomography for bone density assessment. Cureus 2021;13.
28. Pitto R, Bhargava A, Pandit S, Walker C, Munro J. Quantitative CT-assisted osteodensitometry of femoral adaptive bone remodelling after uncemented total hip arthroplasty. Int Orthop 2007;32: 589–95.
29. Shim V, Pitto R, Anderson I. Quantitative CT with finite element analysis: towards a predictive tool for bone remodelling around an uncemented tapered stem. Int Orthop 2012;36:1363–9.
30. Ciliberti FK, Guerrini L, Gunnarsson AE, Recenti M, Jacob D, Cangiano V, et al. CT- and MRI-based 3D reconstruction of knee joint to assess cartilage and bone. Diagnostics 2022;12. Available from: https://www.mdpi.com/2075-4418/12/2/279.
31. Arachchi S, Pitto R, Anderson I, Shim V. Analyzing bone remodeling patterns after total hip arthroplasty using quantitative computed tomography and patient-specific 3D computational models. Quant Imag Med Surg 2015;5:575–82.
32. Magnússon B. Development of clinical assessment strategies for patients undergoing total hip arthroplasty (THA) [Master thesis project]. Reykjavik, Iceland: Reykjavik University; 2013.
33. Pickhardt P, Lauder T, Munoz del Rio A, Bruce R, Binkley N. Opportunistic screening for osteoporosis using abdominal computed tomography scans obtained for other indications. Ann Intern Med 2013;158:588–95.
34. Jang S, Graffy P, Ziemlewicz T, Lee S, Summers R, Pickhardt P. Opportunistic osteoporosis screening at routine abdominal and thoracic CT: normative L1 trabecular attenuation values in more than 20 000 adults. Radiology 2019;291:181648.
35. Marques M, Pereira da Silva N, Heijde D, Reijnierse M, Braun J, Baraliakos X, et al. POS0974 low dose computed tomography hounsfield units: a reliable methodology for assessing changes in vertebral bone density in radiographic axial spondyloarthritis. Ann Rheum Dis 2022;81:792–5.
36. Lim Fat D, Kennedy J, Galvin R, O'Brien F, Mc Grath F, Mullett H. The hounsfield value for cortical bone geometry in the proximal Humerus–An in vitro study. Skelet Radiol 2012;41:557–68.
37. Aamodt A, Kvistad K, Andersen E, Lund-Larsen J, Eine J, Benum P, et al. Determination of hounsfield value for CT-based design of custom femoral stems. J Bone Jt Surg Br 1999;81:143–7.
38. Gerig G, Jomier M, Chakos M. Valmet: a new validation tool for assessing and improving 3D object segmentation. Proc of Med Image Comput Comput-Assisted Intervention (MICCAI'01) 2001:516–28.
39. Bhea B, Guragain H, Kenney-Jung D, Mandrekar J, Watson RE, Welker KM, et al. Segmentation errors and interest reliability in automated and manually traced hippocampal volumes. Ann Clin Transl Neurol 2019;6(9):1807–14.
40. Stöhr K, Phillips C, Healy J, Al-Yassari G, Gibbons CER. Medium-to-long term DEXA analysis of an uncemented (AML) femoral component. HIP Int: J Clin Exp Res Hip Pathol Therapy 2008;18:195–9.
41. Roe S, Marcellin-Little D, Lascelles BDX. Radiographic evaluation of early periprosthetic femoral bone contrast and prosthetic stem alignment after uncemented and cemented total hip replacement in dogs. Vet Surg: VS. 2012;41:902–3.
42. Chandran P, Azzabi M, Andrews M, Bradley J. Periprosthetic bone remodeling after 12 years differs in cemented and uncemented hip arthroplasties. Clin Orthop Relat Res 2011;470:1431–5.
43. Necas L, Hrubina M, Melisik M, Cabala J, Cibula Z, Daniel M. Total hip arthroplasty with ultra-short uncemented stem in patients with osteonecrosis of the femoral head: mid-term results. HIP Int 2023;33: 463–470.
44. Schramm M, Keck F, Hohmann D, Pitto R. Total hip arthroplasty using an uncemented femoral component with taper design: outcome at 10-year follow-up. Arch Orthop Trauma Surg 2000;120:407–12.
45. Digas G, Kärrholm J, Thanner J. Different loss of BMD using uncemented press-fit and whole polyethylene cups fixed with cement: repeated DXA studies in 96 hips randomized to 3 types of fixation. Acta Orthop 2006;77:218–26.
46. Boskey A, Coleman R. Aging and bone. J Dent Res 2010;89:1333–48.
47. Beck B, Snow C. Bone health across the lifespan–exercising our options. Exerc Sport Sci Rev 2003;31:117–22.